

Memory effects in ac hopping conductance in the quantum Hall effect regime: Possible manifestation of DX^- centers

I. L. Drichko,^{1,*} A. M. Diakonov,¹ I. Yu. Smirnov,¹ V. V. Preobrazenskii,² A.I. Toropov,² and Y. M. Galperin^{3,1,†}

¹*A. F. Ioffe Physico-Technical Institute of Russian Academy of Sciences, 194021 St. Petersburg, Russia*

²*Institute of Semiconductor Physics, Siberian division of Russian Academy of Sciences, Novosibirsk, Russia*

³*Department of Physics, University of Oslo, PO Box 1048 Blindern, 0316 Oslo, Norway*

(Dated: November 17, 2018)

Using simultaneous measurements of the attenuation and velocity of surface acoustic waves propagating along GaAs/Al_{0.3}Ga_{0.7}As heterostructures, complex ac conductance of the latter has been determined. In the magnetic fields corresponding to the middles of the Hall plateaus both the ac conductance, $\sigma(\omega)$, and the sheet electron density, n_s , in the two-dimensional conducting layer turn out to be dependent on the samples' cooling rate. As a result, the sample “remembers” the cooling conditions. The complex conductance is strongly dependent on an infrared illumination which also changes both $\sigma(\omega)$ and n_s . Remarkably, the correlation between $\sigma(\omega)$ and n_s is *universal*, i. e. it is independent of the way to change these quantities. The results are attributed to two-electron defects (so-called DX^- centers) located in the Si doped layer.

PACS numbers: 72.20.-i; 72.30.+q; 72.50.+b; 73.43.-f; 73.63.-b

I. INTRODUCTION

As well known,¹ in the quantum Hall effect (QHE) regime magnetic field dependences of off-diagonal, σ_{xy} , and diagonal, σ_{xx} , components of dc conductivity tensor are very much different. Namely, σ_{xy} shows a set of flat plateaus with abrupt steps taking place at half-integer values of the filling factor $\nu = 2\pi n_s a_H^2$ where n_s is sheet density of two-dimensional electron gas (2DEG) while $a_H = (\hbar c/eH)^{1/2}$ is the quantum magnetic length. On the contrary, $\sigma_{xx}^{(dc)}$ is extremely small at the plateaus and has sharp maxima at the steps between the Hall plateaus, i. e. at *half-integer* filling factors. The conventional explanation is that at a half-integer ν electronic states the Fermi level are *extended* while apart of the half-integer values of ν they are *localized*.

A powerful way to investigate the interplay between extended and localized states is an analysis of *ac* conductivity by acoustical methods.² A surface acoustic wave (SAW) propagating in a vicinity of a 2DEG layer produces a wave of electric field penetrating the 2DEG. This wave creates currents which, in turn, produce a feedback to the SAW. As a result, both SAW attenuation Γ and velocity V depend on the properties of the 2DEG. In particular, simultaneous measurements of attenuation and velocity of SAW provide a unique possibility to determine *complex* ac conductivity, $\sigma_{xx}(\omega) = \sigma_1(\omega) - i\sigma_2(\omega)$, as a function of external magnetic field H and SAW frequency ω . Furthermore, the magnetic field dependence of complex conductivity provides an information both on the extended and localized states, as well as on metal-to-insulator transition.

As we observed earlier,^{3,4} near the steps on Hall conductance, i. e. at half-integer ν , imaginary part of the complex ac conductance is small while its real part coincides with the dc transverse conductance, $\sigma_{xx}^{(dc)}$. However, in the magnetic fields corresponding to regions near the

middles of the Hall plateaus, i. e. at small integer ν , the difference between $\sigma_{xx}(\omega)$ and $\sigma_{xx}^{(dc)}$ turns out to be crucial. Namely, $\sigma_{xx}^{(dc)}$ is extremely small while both $\sigma_1(\omega)$ and $\sigma_2(\omega)$ are measurable quantities and $\sigma_2(\omega) \gg \sigma_1(\omega)$. Furthermore, up to our experimental accuracy, the dissipative conductivity, $\sigma_1(\omega)$ is proportional to SAW frequency and weakly dependent on the temperature. According to Ref. 5, these facts lead to the conclusion that the mechanism of ac conductance is *hopping*.

In our experiment, the SAW is induced by inter-digital transducers at the surface of a piezoelectric LiNbO₃ plate. Samples are layered structures placed on the plate, so the interface layer is located at some distance from the piezoelectric surface. If the conductance of the interface layer is low, then the ac electric field produced by the SAW decays as $\sim e^{-k|z|}$ where $k = \omega/V$ is the SAW wave vector while z is the distance from the propagation surface. In the following we assume that both the piezoelectric plate and the samples' layers are parallel to the xy -plane and magnetic field \mathbf{H} is directed along z -axis. Consequently, it is the region of the thickness $\approx k^{-1}$ that contributes to acoustic properties of the system. However, a perfectly conducting layer placed at a distance $\ll k^{-1}$ above the surface *screens* the ac electric field and confines the electric current inside the layer. As a result, in this case both SAW attenuation and velocity are determined mostly by the processes inside the interface layer. An estimate for the dimensionless parameter discriminating between the cases of weak and strong screening is the ratio $|\sigma_{xx}|/V$. Since σ_{xx} is a strong function of magnetic field, variation of the magnetic field changes the screening of the ac electric field. As a result, at different magnetic fields different layers of the sample provide the dominant contribution to $\sigma_{xx}(\omega)$. In particular, at the Hall plateaus “shunting” of the interface layer by a doped one can be dominant. A more detailed analysis⁶ for Si δ -doped GaAs/Al_{0.3}Ga_{0.7}As heterostructures has

shown that it is the case. Namely, at the Hall plateaus the doped layer's contribution to $\sigma_1(\omega)$ turns out to be important. At the same time, its contribution to the dc transverse conductance remains negligibly small.

A procedure outlined in Ref. 6 allowed us to separate the contribution in the ac conductance in QHE regime of the interface layer and the doped layer using their different magnetic field dependences. What we found is that the second contribution significantly fluctuates from one experimental run to another. A preliminary analysis has lead us to a conclusion that what we observe is a *systematic* dependence on cooling procedure rather than random fluctuations - the sample somehow “remembers” the experiment preparation conditions. Furthermore, the doped layer contribution appears also sensitive to the sample illumination.

The aim of the present paper is a systematic study of the “memory effects” in Si δ -doped and modulated doped GaAs/Al_{0.3}Ga_{0.7}As heterostructures by the acoustic method for different cooling and illumination procedures. We will show that both the ac conductivity $\sigma_{xx}(\omega)$ and sheet electron density in the interface layer, n_s , are influenced by the above mentioned procedures. However, in a rather wide region of parameters there exists a *universal* correlation between $\sigma_1(\omega)$ and n_s irrespectively of the way to produce a given n_s . A consistent qualitative explanation of the observed phenomena can be achieved by a suggestion that the memory effects are due to the so-called DX^- centers^{7,8} which are two-electron localized states bound by a negative correlation energy, see, e. g., Ref. 9 for a review.

The paper is organized as follows. In Sec. II experimental procedure and main results are described. These results are discussed in Sec. III, the conclusions are drawn in Sec. IV.

II. EXPERIMENT

A. Experimental setup

A SAW has been induced in a LiNbO₃ crystal on top of which the sample has been placed and fixed by a spring. Details of experimental setup are given in Ref. 3. Its important feature is that there is no direct mechanical coupling between the LiNbO₃ substrate and the sample because some finite clearance. Consequently, only electrical coupling is present that makes determining of $\sigma_{xx}(\omega)$ simpler and more reliable.

Simultaneous measurements of the attenuation, Γ , and relative variation of the sound velocity, $\Delta V(H)/V$ of SAWs in the frequency range $f = \omega/2\pi = 30 - 150$ MHz were performed in magnetic fields up to 7 T at two temperatures 4.2 and 1.5 K. Two sorts of MBE grown GaAs/Al_{0.3}Ga_{0.7}As heterostructures we studied: (i) Si δ -doped with $n_s \approx (1.3 - 4) \times 10^{11} \text{ cm}^{-2}$ and (ii) Si modulated-doped heterostructures with $n_s \approx (2.4 - 7) \times 10^{11} \text{ cm}^{-2}$. The electron densities were determined from

the periods of Shubnikov-de Haas-type oscillations of Γ and $\Delta V/V$ at 4.2 and 1.5 K. The structure of the samples is schematically shown in Fig. 1

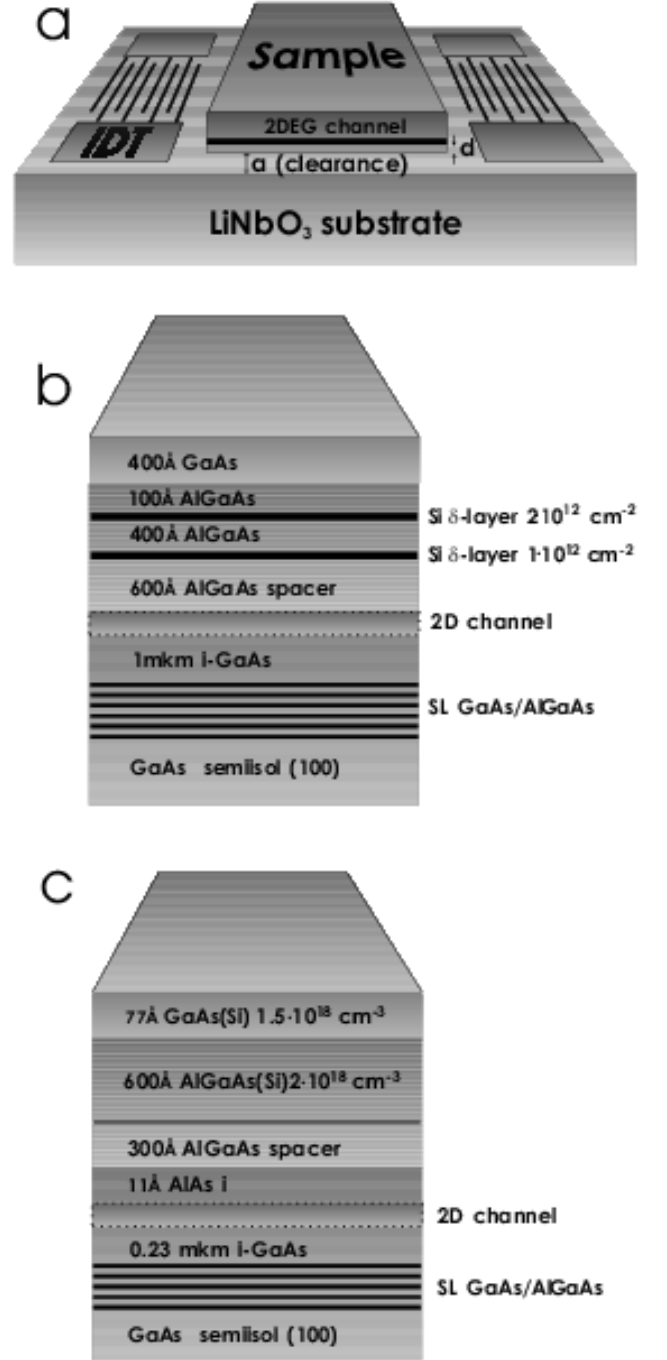


FIG. 1: (a) Three-layers model used to extract ac conductance from acoustical data; Schematic structures of a Si δ -doped sample with $n_s \approx 1.5 \times 10^{11} \text{ cm}^{-2}$ (b), and a modulated-doped one with $n_s \approx 2.4 \times 10^{11} \text{ cm}^{-2}$ (c).

The heterostructure was considered as a multilayer system containing a thin conductive layer with complex

sheet conductance $\sigma_{xx}(\omega)$ at some distance d from the bottom plane. Since the distance between the interface and the doped layer is much less than the SAW penetration depth k^{-1} the quantity $\sigma_{xx}(\omega)$ is actually the *effective conductance* of the region including interface and doped layers, connected “in parallel”. Dielectric constants of two other layers (GaAs and $\text{Al}_{0.3}\text{Ga}_{0.7}\text{As}$, respectively) are assumed to be equal and denoted as $\varepsilon_s = 12$. The heterostructure is placed on top of the LiNbO_3 platelet with effective dielectric constant $\varepsilon_p = 50$, the vacuum clearance between the heterostructure and the plate being denoted as a . The clearance remains finite despite of the fact that the heterostructure was pressed to the piezoelectric platelet because of some roughness of both surfaces. Since the actual clearance is hardly controlled, the quantity a is treated as an adjustable parameter. It is determined by fitting the experimental data at the steps between the Hall plateaus where the conductance is metallic and essentially frequency independent in the frequency region of our experiments. The values of a are slightly different for different sample setups. For our experimental setup, $a \approx (1 - 5) \times 10^{-5}$ cm.

According to the above model, components of the complex conductivity have been extracted from the experimental data from the expressions⁶

$$\Gamma = 4.34kA(k)K^2 \frac{\Sigma_1}{(1 + \Sigma_2)^2 + \Sigma_1^2}, \text{ dB/cm}, \quad (1)$$

$$\frac{\Delta V}{V} = 0.5A(k)K^2 \frac{1 + \Sigma_2}{(1 + \Sigma_2)^2 + \Sigma_1^2}, \quad (2)$$

$$\Sigma_{1,2} = 4\pi t(k)\sigma_{1,2}(\omega)/\varepsilon_s V. \quad (3)$$

Here K is the electromechanical coupling constant for LiNbO_3 (Y-cut), $A(k)$ and $t(k)$ are dimensionless functions allowing for electrical and geometrical properties of the sample,⁶

$$\begin{aligned} A(k) &= 8(\varepsilon_p + 1)\varepsilon_s e^{-2k(a+d)} / (b_1(k)[b_2(k) - b_3(k)]), \\ t(k) &= [b_2(k) - b_3(k)]/2b_1(k), \\ b_1(k) &= (\varepsilon_p + 1)(\varepsilon_s + 1) - (\varepsilon_p - 1)(\varepsilon_s - 1)e^{-2ka}, \\ b_2(k) &= (\varepsilon_p + 1)(\varepsilon_s + 1) - (\varepsilon_p + 1)(\varepsilon_s - 1)e^{-2kd}, \\ b_3(k) &= e^{-2ka}[(\varepsilon_p - 1)(\varepsilon_s - 1) + (\varepsilon_p - 1)(\varepsilon_s + 1)e^{-2kd}]. \end{aligned}$$

B. Dependence of cooling rate

The acoustic measurements require the sample to be placed either in vacuum, or in a dilute gas. Otherwise SAW are strongly damped by the cooling liquid. In our experiment, the system consisting of the sample mounted on the LiNbO_3 plate was placed on a cooling finger located in a chamber. The chamber was, in turn, placed in a He^4 cryostat which can be pumped out to decrease its temperature. The superconductor solenoid in the cryostat was cooled by liquid nitrogen. To reach the temperatures 1.5–4.2 K a dilute exchange gas (He^4 , ~ 0.1 Torr) was inserted into the chamber, and that was the way to control the cooling rate.

The cooling procedure was as follows. The chamber containing the experimental setup has been initially cooled inside the cryostat by cold gaseous He^4 , and then liquid He has been poured into the cryostat.

Different cooling regimes were studied, and in the following they will be referred to as *slow* and *rapid* cooling. In the first case the exchange gas has been inserted from the very beginning, at the room temperature. Then the chamber was cooled during 1.5 - 2 hours by cold gaseous He^4 down to 7 - 8 K, and finally liquid He was poured. In the second case, the chamber was initially evacuated and cooled first by gaseous and then by liquid He^4 , the sample temperature being monitored by a carbon thermometer. At some temperature T_0 , which actually depends on the pressure in the chamber, the exchange gas was inserted, and the sample cooled down to the cryostat temperature during 5-10 minutes. As a result, the cooling rate is an increasing function of T_0 , the maximum cooling rate being at $T_0 \approx 77$ K.

The results for a slowly-cooled of the Si δ -doped sample with the initial sheet electron density $n_s \simeq 1.5 \times 10^{11} \text{ cm}^{-2}$ are shown in the bottom panel of Fig. 2. They are extracted from the raw data shown in the top panel.

Magnetic field dependences for different cooling rates extracted at the same acoustic frequency, $f = 30$ MHz, are shown in Fig. 3. One can observe that, depending on T_0 , (i) minimum values of σ_1 are different, and (ii) minima occur at different values of magnetic field. Since all the minima correspond to the filling factor $\nu = 2$, it follows that the sheet electron density, n_s , is a function of T_0 . The behavior of σ_1 for $\nu = 1$ and $\nu = 4$ is similar.

In Fig. 4, the values of $\sigma_1|_{\nu=2}$ and $n_s|_{\nu=2}$ are plotted versus the pre-cooling temperature, T_0 . The first quantity increases with increase of T_0 , while the second one decreases. For all T_0 , imaginary part of the conductivity, σ_2 , remains greater than σ_1 that indicates hopping conductance. σ_2 is also dependent on T_0 , however its dependence is much slower than that of σ_1 . The general behavior of the ac conductance in the modulated-doped samples is similar.

The dependence of the sheet electron density n_s turns out to be correlated with the *initial* value of n_s ; the larger the initial n_s the slower its dependence on T_0 . For the sample with $n_s \simeq 1.5 \times 10^{11} \text{ cm}^{-2}$ the relative variation of n_s is 30%, for $n_s \simeq 2.3 \times 10^{11} \text{ cm}^{-2}$ is 10%, while $n_s = 7 \times 10^{11} \text{ cm}^{-2}$ the dependence on T_0 is essentially absent. In the last sample the first band of size quantization is almost full.

It is worth noting that the state reached by fast cooling does not change for a long time. In particular, characteristics of the sample with $n_s = 1.2 \times 10^{11} \text{ cm}^{-2}$ after maximally fast cooling from $T_0 = 77$ K did not change during at least 28 hours.

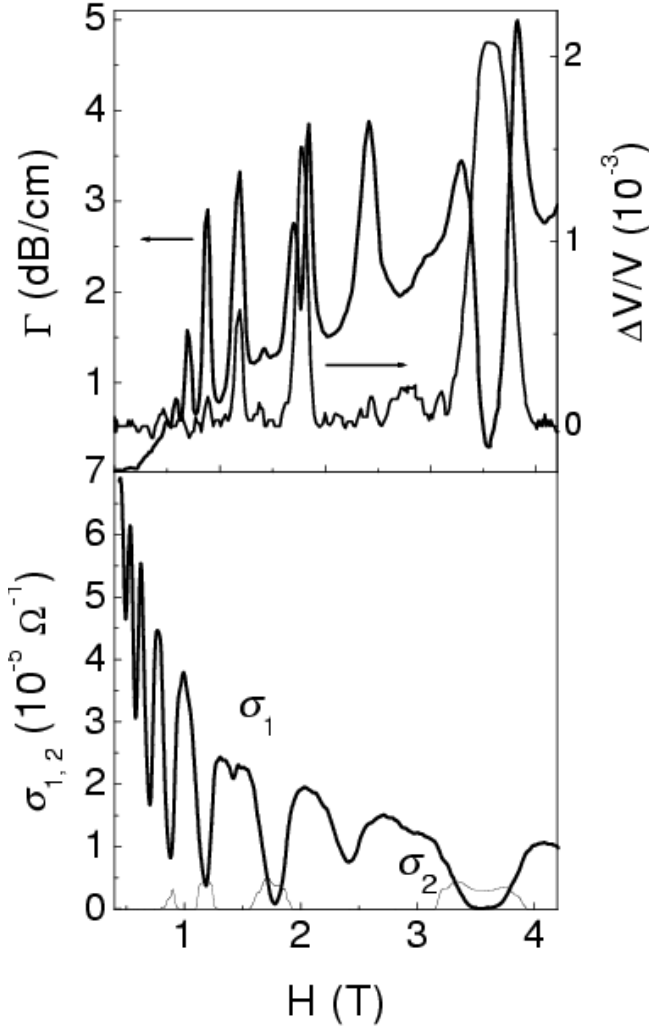


FIG. 2: Top panel: magnetic field dependences of the SAW attenuation, Γ , and of the relative velocity change, $\Delta V/V$ for $f = 30$ MHz. Bottom panel: components σ_1 and σ_2 of ac conductivity versus magnetic field H at $T = 1.5$ K. Sample – Si δ -doped GaAs/Al_{0.3}Ga_{0.7}As heterostructure, initial electron density $n_s \simeq 1.5 \times 10^{11} \text{ cm}^{-2}$.

C. Dependence on illumination

As well known, dc conductance of Al_{0.3}Ga_{0.7}As thin film⁷ and GaAs/Al_{0.3}Ga_{0.7}As heterostructures¹⁰ is sensitive to infrared (IR) illumination. To investigate combined effect of slow cooling and IR illumination on ac conductance light emitting diodes (LEDs) producing IR radiation with the wavelength $\lambda = 0.81, 1.34, 2.53$ and $4.47 \mu\text{m}$ were placed into the chamber¹¹. Choosing the illumination dose we were able to change the sheet electron density, as well as the ac conductance, by controllable portions. The persistent ac photoconductance is observed only if the illumination frequency exceeds some threshold located between 0.92 and 0.49 eV ($\lambda = 1.34$

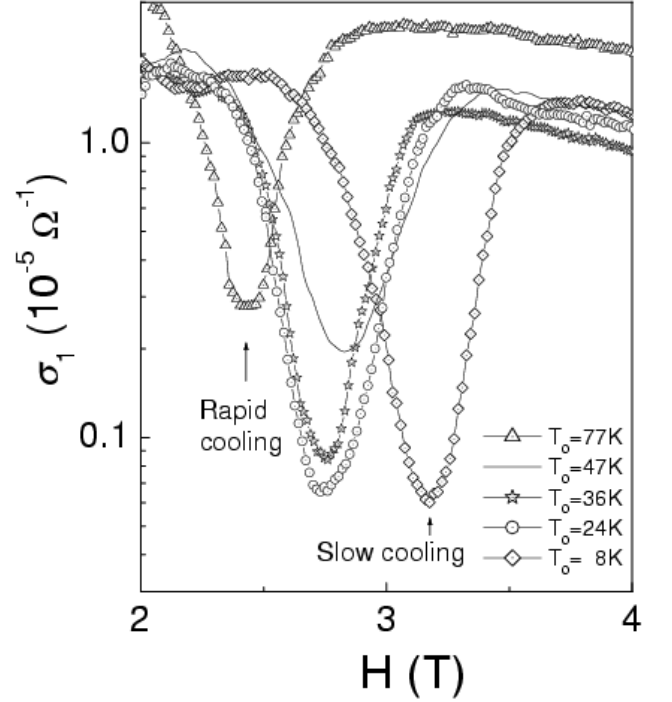


FIG. 3: Magnetic field dependences of σ_1 for $T = 1.5$ K, $H = 2 - 4$ T and different pre-cooling temperatures, T_0 . All curves correspond to the filling factor $\nu = 2$.

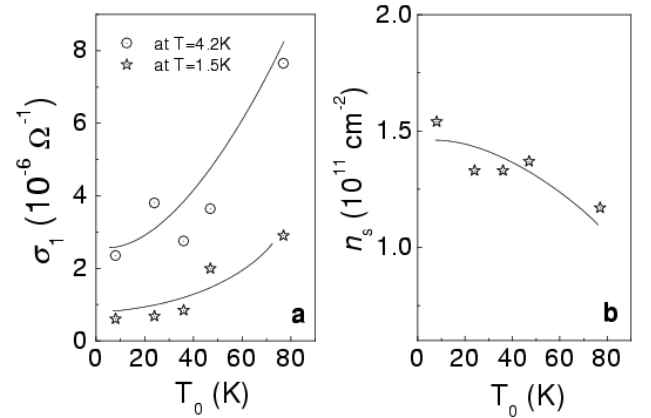


FIG. 4: Dependences of the ac conductance σ_1 (left panel) and sheet electron density n_s (right panel) on the pre-cooling temperature T_0 . $\nu = 2$, temperatures of experiment are shown in the legend.

and $2.53 \mu\text{m}$, respectively). The magnetic field dependence of $\sigma_1(\omega)$ after successive illumination of a δ -doped sample with $n_s \simeq 3.3 \times 10^{11} \text{ cm}^{-2}$ is shown in Fig. 5. One can see that successive pulsed illumination (pulse duration $\lesssim 10$ s) leads to a shift in the location of the corresponding σ_1 minimum. The shift indicates an *increase* in the 2DEG density, n_s . At the same time the minimum value of σ_1 *decreases*. The effect of the illumination in a Si doped structure is illustrated in Fig. 6. Here $\sigma_1(\omega)$

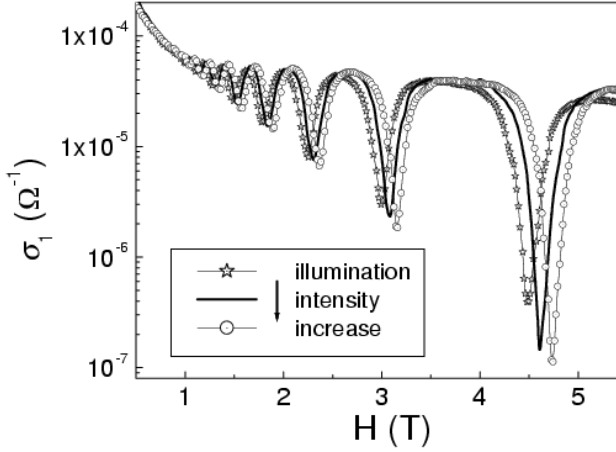


FIG. 5: Magnetic field dependences of $\sigma_1(\omega)$ after successive illumination, $\lambda = 0.81 \mu\text{m}$, $T = 4.2 \text{ K}$, $f = 30 \text{ MHz}$.

and $\sigma_2(\omega)$ are plotted as functions of the sheet electron density n_s , tuned by successive illumination. All three quantities are extracted from acoustic measurements at $T = 1.5 \text{ K}$. One can see that increase in n_s is accompanied by decrease of σ_1 down to some value after which a rapid increase occurs. In this regime the successive illumination leads to an increase in σ_1 leaving n_s almost constant.

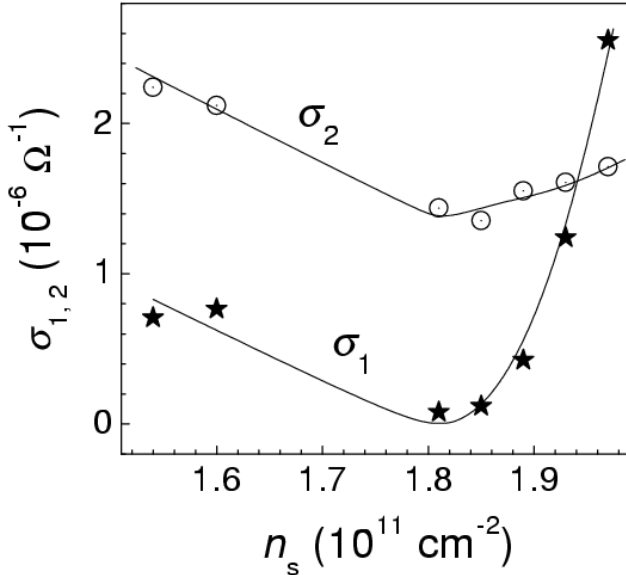


FIG. 6: Effect of illumination presented as $\sigma_{1,2}$ versus n_s curves. Each point corresponds to a state after a given illumination dose, $\nu = 2$.

III. DISCUSSION

As we expected,⁶ the set of experimental results indicates a significant role of the doped layer in the “memory” effects. Indeed, a remarkable feature of the experimental results is that, being presented as σ_1 and σ_2 versus n_s , they are more-or-less universal. Namely, the data obtained for different cooling and illumination procedures *collapse* to almost same curves. To demonstrate this feature, in Fig. 7 we plot σ_1 and σ_2 versus n_s for a Si δ -doped sample with initial electron concentration $n_s \simeq 1.5 \times 10^{11} \text{ cm}^{-2}$. Here the results both for different pre-cool temperatures T_0 and different illumination doses are included. We believe that such prop-

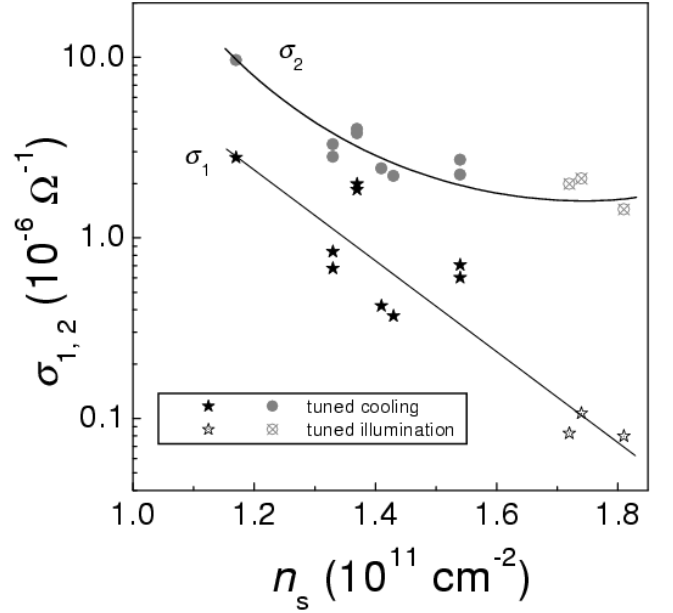


FIG. 7: Combined effect of cooling and successive illumination for $\sigma_1(\omega)$ and $\sigma_2(\omega)$ which are plotted versus n_s tuned either by fast cooling, or by illumination. δ -doped sample, $n_s \simeq 1.5 \times 10^{11} \text{ cm}^{-2}$, $T = 1.5 \text{ K}$. Measurements are performed at $f = 30 \text{ MHz}$; $\nu = 2$.

erty, as well as the threshold in ac photoconductance support the idea that the electron states in the doped layer are just the so-called DX^- centers.⁷ These states are actually two-electron bound states stabilized by local lattice distortion. DX^- centers were observed both in $\text{GaAs}/\text{Al}_{0.3}\text{Ga}_{0.7}\text{As}$ heterostructures and in $\text{Al}_x\text{Ga}_{1-x}\text{As}$ films with $x > 0.22$. They are considered to be responsible for dc persistent photoconductance in these systems, which has also a threshold in the illumination quanta energy located between 0.6^7 and 0.8 eV^{12} .

In general, the defects responsible for the DX^- centers have three charge states which differ by number of electrons occupying the center. Due to a local lattice distortion the two-electron state has the lowest energy if the two electron correlation energy $|U|$ exceeds the thermal energy kT .¹³ As a result, at $T \ll |U|/k$ the de-

fects are either occupied by two electrons and negatively charged (D_- -centers) or empty and positively charged (D_+ -centers). The D_- -centers can be treated as *small bipolarons*. The real situation is more complicated than the one discussed above since there is no unique opinion on the microscopic nature of excited states of the defect. In particular, there are several intermediate states of the defect each containing one electron, but differing by the amount of lattice distortion. In the following we will not discriminate between these states since detailed theory of acoustically-stimulated electron tunneling is beyond the scope of the present work. To simplify the discussion, following Ref. 14, we assume that a set of equal number of D_- and D_+ states form the ground state which is the only state occupied at very low temperature. The one-electron (neutral) state D_0 has the energy higher than the ground state energy by the correlation energy $o|U|$.

In heterostructures, one can imagine several processes taking place during a cooling from the room temperature to 1.5 K. Among them are freeze-out of the carriers in the Si-doped layer of $\text{Al}_{0.3}\text{Ga}_{0.7}\text{As}$ to occupy first deep D_- states and then shallow states,¹⁵ carriers exchange between the doped and the interface layers, etc. We believe that under rapid cooling the electron distribution at the pre-cooling temperature T_0 is frozen - it does not significantly change during the cooling below T_0 . This statement is compatible with a crude estimate of the activation energy based on the expression $E_d \approx 0.7x - 0.15$ eV which has been obtained for $\text{Al}_x\text{Ga}_{1-x}\text{As}$ films for $0.22 < x < 0.4$.¹⁵ For our samples, this estimate yields $E_d = 60$ meV. Consequently, $e^{-E_d/kT}$ varies from 10^{-1} to 10^{-4} as T varies from 300 to 100 K.

Acoustic methods under conditions of the QHE provide a unique possibility to separate the contributions of the interface and doped layers. Indeed, at the QHE plateaus the electronic states in the interface layer are *localized*, and their contribution to σ_{xx} are small. As a result, the contribution of the electron hopping in the *doped layer* becomes measurable.⁶ We believe that the main mechanism leading to this contribution is due to tunneling transition of electron pairs (bipolarons) between a D_- center and an adjacent D_+ one. At low temperatures sequential tunneling via the neutral states D_0 is probably not important since the energy difference between D_0 and the ground state is of the order of $|U| \approx 1$ eV. However, D_0 states play an important role in the formation of the tunneling barrier between D_- and D_+ centers. A theory of ac hopping conductance due to DX^- -centers in three-dimensional amorphous materials has been developed in Ref. 14. According to this theory, it is rather difficult to discriminate between single-electron and two-electron tunneling from frequency and temperature dependences of $\sigma(\omega)$. We are not aware of a theory of ac hopping conductance relevant to pair tunneling in $\text{GaAs}/\text{Al}_{0.3}\text{Ga}_{0.7}\text{As}$ heterostructures. However, one can expect that the differences in frequency and temperature dependences are very small also in this case.

Assuming that the doped layer's thickness is much less

than k^{-1} we can use for σ_1 an estimate similar to the well-known expression for the single-electron tunneling,⁵

$$\sigma_1(\omega) \sim g_b^2 \xi_b^3 \omega e^4 / \varepsilon_s.$$

Here g_b is the density of states for bipolarons, ξ_b is their localization length, while e is the electron charge. We believe that it is the density of D_- states, g_b , that is influenced by cooling and illumination procedures. In particular, the IR illumination causes ionization of the D_- centers in the doped layer. Part of released electrons tunnels into the interface layer that results in the increase in the sheet density n_s . A similar effect occurs during a rapid cooling due to quenching of the electron transfer between the defects and 2D layer. The higher the pre-cooling temperature T_0 the less time left for the electrons to tunnel into the interface layer. As a result, n_s is a decreasing function of T_0 .

It worth mentioning that there is an important difference between the dc persistent photoconductance and the effect we observe. Indeed, in the first case the conductance is possibly due to extended electron states either in the 2DEG-layer or in the conduction band in $\text{Al}_{0.3}\text{Ga}_{0.7}\text{As}$ layer. Contrary, the states responsible for the ac conductance are *localized* that follows from the relation $\sigma_2(\omega) \gtrsim \sigma_1(\omega)$. Illumination leads to a *decrease* in the number of occupied bound states. As a result, the ac conductance decreases with illumination. At very high illumination dose the DX^- centers become ionized, and all the ac conductance is due to extended states.

We have employed the procedure of Ref. 6 to separate the contributions of the doped layer and of the 2D layer in the ac hopping conductance and then analyzed the latter using a picture of single electron nearest-neighbor tunneling. Tuning the 2DEG density by illumination after slow cooling to change the magnetic field H corresponding $\nu = 2$ from 2.7 to 3.8 T we have found that the localization length ξ in this region behaves as $H^{-1/2}$. This dependence is compatible with the assumption of the single electron nearest neighbor tunneling. Unfortunately, we were not able to carry out a similar analysis for $\nu = 4$ since at large ν the components σ_1 and σ_2 are of the same order of magnitude, and the mechanism of ac conductance is mixed.

IV. CONCLUSIONS

Main conclusions from the present work can be formulated as follows.

- (i) Both ac hopping conductance and sheet electron density in Si δ -doped and modulation doped $\text{GaAs}/\text{Al}_{0.3}\text{Ga}_{0.7}\text{As}$ heterostructures at the quantum Hall effect plateaus depend on the samples' *cooling rate*.
- (ii) Successive IR illumination leads to a *persistent ac hopping photoconductance* which decreases with the

illumination dose. At the same time, the sheet electron concentration, n_s , in the interface layer increases. The persistent ac photoconductance occurs only if the illumination frequency exceeds some threshold located between 0.5 and 0.9 eV.

- (iii) The above set of results can be qualitatively interpreted within the framework of the concept of DX^- centers – localized two-electron states bounded by local lattice distortion – located in the doped layer of the heterostructure. We believe that the doped layer ac hopping conductance is due to tunneling of electron pairs (bipolarons) between adjacent doubly occupied and empty defects.
- (iv) The contribution of tunneling between localized

states in the interface layer can be extracted and used to estimate the electron localization length, ξ . Within the experimentally-accessible range, $\xi \propto H^{-1/2}$ which is compatible with single-electron nearest neighbor tunneling.

Acknowledgments

One of the authors (ILD) is thankful B. A. Volkov and D. R. Khokhlov for discussions. The work is supported by RFFI 01-02-17891, MinNauki, Presidium RAN grants and Russia-Ukraine Program *Nanophysics and Nanoelectronics*.

* Electronic address: Irina.L.Drichko@pop.ioffe.rssi.ru

† Electronic address: iouri.galperine@fys.uio.no

- ¹ The Quantum Hall Effect, ed. by R. E. Prange and S. M. Girvin (Springer-Verlag, New York 1987).
- ² A. Wixforth, J. Scriba, M. Wassermeier, J. P. Kotthaus, G. Weimann, and W. Schlapp, Phys. Rev. B **40**, 7874 (1989). R. L. Willett, R. R. Ruel, K. W. West, and L. N. Pfeiffer, Phys. Rev. Lett. **71**, 3846 (1993). A. Schenstrom, Y. J. Quian, M. F. Xu, H. P. Baum, H. Levy, and B. K. Sarma, Sol. State Comm. **65**, 739 (1988).
- ³ I. L. Drichko, A. M. D'yakonov, A. M. Kreshchuk, T. A. Polyanskaya, I. G. Savel'ev, I. Yu. Smirnov and A. V. Suslov, Fiz. Tekh. Poluprov. **31**, 451 (1997) [Semiconductors **31**, 384 (1997)].
- ⁴ I. L. Drichko, A. M. D'yakonov, V. D. Kagan, I. Yu. Smirnov, and A. I. Toropov, Proc. of 24th ICPS, Jerusalem, on CD-ROM (1998).
- ⁵ A. L. Efros, Zh. Eksp. Teor. Fiz. **89**, 1834 (1985) [JETP **89**, 1057 (1985)].
- ⁶ I. L. Drichko, A. M. Diakonov, I. Yu. Smirnov, Y. M. Galperin, and A. I. Toropov, Phys. Rev. B **62**, 7470 (2000).
- ⁷ D. V. Lang, R. A. Logan, Phys. Rev. Lett. **39**, 635 (1977).
- ⁸ D. J. Chadi and K. J. Chang, Phys. Rev. B **39**, 10063 (1989).

⁹ P. M. Mooney, J. Appl. Phys. **67**, R1 (1990).

- ¹⁰ E. Buks, M. Heiblum, and Hadas Shtrikman, Phys. Rev. B **49**, 14790.
- ¹¹ N. V. Zotova, S. A. Karandashev, B. A. Matveev, A. V. Pentsov, S. V. Slobodchikov, N. N. Smirnova, N. M. Stus', G. N. Talalakin, and I. I. Markov. Optoelectronic sensors based on narrow band A3B5 alloys, SPIE 1587 Chemical, Biochemical and Environmental Fiber Sensors III. pp. 334-345, Boston 1991.
- ¹² A. E. Beljaev, Kh. Yu. von Bardeleben, E. I. Oborina, Yu. S. Riabchenko, A. I. Savchuk, M. L. Fije, M. K. Sheinkman, Fiz. Tekh. Poluprov. **28**, 1544 (1994) [Semiconductors **28**, 1544 (1994)].
- ¹³ Since the lattice distortion stimulates an *attraction* of two electrons at the center, the correlation energy U is *negative*. Sometimes U is called the Hubbard energy, and DX^- centers are referred to as the centers with negative Hubbard energy.
- ¹⁴ M. Foygel, A. G. Petukhov, A. S. Andreyev, Phys. Rev. B **48**, 17018 (1993).
- ¹⁵ N. Chand, T. Henderson, J. Klem, W. T. Masselink, Russ Fisher, Yia-Chung Chang, H. Morkoc, Phys. Rev. B **30**, 4481 (1984).